Journal of Experimental Nanoscience
Publication details, including instructions for authors and subscription information:
http://www.informaworld.com/smpp/title~content=t716100757

High efficiency solution infiltration routes to thin films with photonic properties

L. Zhou[a]; D. S. Boyle[a]; K. Govender[a]; P. O'brien[a]
[a] The Manchester Materials Science Centre and Department of Chemistry, University of Manchester, Manchester, UK

To cite this Article Zhou, L. , Boyle, D. S. , Govender, K. and O'brien, P.(2006) 'High efficiency solution infiltration routes to thin films with photonic properties', Journal of Experimental Nanoscience, 1: 2, 221 — 233
To link to this Article: DOI: 10.1080/17458080600622107
URL: http://dx.doi.org/10.1080/17458080600622107

Journal of Experimental Nanoscience,
Vol. 1, No. 2, June 2006, 221–233

Taylor & Francis
Taylor & Francis Group

High efficiency solution infiltration routes to thin films with photonic properties

L. ZHOU, D. S. BOYLE, K. GOVENDER and P. O'BRIEN*

The Manchester Materials Science Centre and Department of Chemistry, University of Manchester, Oxford Road, Manchester, UK

(*Received October 2005; in final form February 2006*)

A chemical bath deposition (CBD) method has been developed to prepare three-dimensionally-ordered macroporous films of CdS and TiO_2, using colloidal crystals as templates. A series of sequential, short infill/rinse/anneal steps are employed to effect complete infiltration of SiO_2 (opal) thin films with CdS or TiO_2. Removal of templates allows fabrication of macroporous inverse replica structures that exhibit periodic modulation of dielectric behaviour and have potential for use in photonic applications. A study of the photonic properties of films indicates that the multi-step CBD method is a useful approach for infiltration of opal interstices.

Keywords: CBD; Infiltration; Inverse opals

1. Introduction

The fabrication of ordered macroporous materials (*i.e.* pore diameters greater than 50 nm) has become a rapidly growing field in recent years [1]. This development is due to their wide range of potential applications including use as separation media [2, 3], novel catalysts [4, 5] and more recently as photonic crystals [6–8]. Photonic crystals are structures with three-dimensional periodicity generally on a length scale comparable to that of electromagnetic radiation encompassing the IR-visible-UV region. Photonic structures have potential for use in optical processing devices, such as miniature waveguides, mirrors in optical circuits directing light photons, in general developing analogs to conductors and insulators used to direct the passage of electrons in conventional electronic circuits [6].

Many methods have been developed to fabricate macroporous structures, generally described as either "top-down" or "bottom-up" approaches. The former include micromachining methods, which require complicated and expensive apparatus. The latter, which include "soft-chemical" approaches such as colloidal self-assembly

*Corresponding author. Email: paul.obrien@manchester.ac.uk

Journal of Experimental Nanoscience
ISSN 1745–8080 print/ISSN 1745–8099 online © 2006 Taylor & Francis
http://www.tandf.co.uk/journals
DOI: 10.1080/17458080600622107

and templating methods, have significant advantages for the experimentalist such as lower capital costs and use of simple synthetic procedures. By these methods, colloidal crystals are synthesised and used as inverse templates for the final structure; voids between the colloidal particles comprising the crystal can be infiltrated by a second phase using vapour or liquid infusion methods. Upon removal of the colloidal template, by thermal or chemical methods, a porous periodic structure may be formed. A variety of macroporous materials have been synthesised using this procedure, including polymers [9, 10] semiconductors [5, 8] and metals [11–13].

Whilst the process of colloidal self-assembly and template construction has been well developed, the infiltration process remains problematic and no general procedure has gained widespread application. Vapour phase methods such as Atomic Layer Deposition [14] have been shown to be effective but require specialised apparatus and are not generally applicable. During infiltration, continuous formation of solid phase tends to reduce and ultimately close porosity at the extremities of the structure, impeding the inflow of reactive precursors and removal of reaction by-products. Both processes compromise the efficacy and are common to all infiltration methods. Solution infiltration methods include sol-gel processing [15–17], UV-induced polymerization [10], particle infusion [18] and electrodeposition [13, 19, 20]. The choice of infiltration method used is largely a function of the nature of both the colloidal template and infill material. Factors such as the effects of dynamic change in pore volume (*i.e.* pore size and contact angle will progressively decrease) and resultant modulation of capillary forces, which draw the precursor through the porous solid as reaction proceeds, are also important.

Aqueous solution deposition methods, such as chemical bath deposition (CBD) and variants thereof, can provide economic and efficient approaches to thin film materials, in particular metal oxides and chalcogenides. Many of these compounds are semiconductors with large refractive indices and electronic bandgaps, a prerequisite for photonic applications. In addition to issues mentioned previously, a further factor that requires attention when producing porous compound semiconductors by solution methods is the electrochemical properties of the solution and templates. As a result of the influence of electrostatic forces and surface chemistry, a colloidal template covered with a progressively growing semiconductor surface in contact with an electrolyte solution will develop a surface charge, which in turn promotes the formation of a tightly bound inner layer of opposite charge (Stern or Helmholtz layer). The inner layer attracts a cloud of counterions and hence a so-called ''diffuse double-layer'' is produced, whose magnitude is dependent mainly in the ionic strength of the solution. Hence the local chemical environment is strongly perturbed which may lead to modification of the growth kinetics.

A successive CBD method has been successfully used to prepare macroporous CdS [21] and Sb_2S_3 [22] films. The colloidal crystal template is immersed first in a solution containing the metal cation, rinsed, then immersed in a solution containing the desired anion, and again rinsed. The process is then repeated for as many times as needed to infill the interstices of the opal. Upon removal of template, highly ordered macroporous films can be obtained. This method is usually called successive ion-layer adsorption and reaction (SILAR). The reaction mechanism is different to conventional CBD methods and in general film growth is slow and tedious. The variety of products is also limited

as compared to conventional CBD methods, which have been studied for almost 150 years and by which a vast array of different semiconductors films have been prepared [23]. We have previously described the growth of metal sulfide films (CdS [24–26], ZnS [27, 28] and In_2S_3 [29]) and metal oxides (ZnO [30–34]) from basic and acidic solution. To the best of our knowledge, there have been no reports on the preparation of macroporous films using the conventional CBD method.

In this paper we demonstrate a new strategy by which conventional single-bath CBD can be used to fully infill the interstices of opals. We describe a universal strategy to infiltrate macroporous colloidal templates, formed from monodispersed polystyrene (PS) and SiO_2 colloids, with TiO_2 or CdS by solution deposition methods. Moreover, due to the similarity of solution deposition methods, this strategy has universal applicability for preparation of macroporous films by single-bath CBD methods and other chemical solution methods.

2. Experimental

2.1. *Preparation of colloidal crystal template layers*

Polystyrene (PS) latex beads (mean particle size 460 nm) were obtained commercially (Sigma-Aldrich) and employed without further treatment. Monodisperse silica (SiO_2) colloids were synthesized following a procedure adapted from Stöber [35]. The morphology and polydispersity of the particles was determined by TEM; silica spheres with diameter 435.5 nm ($\pm$11.5 nm) and 523.5 nm ($\pm$11.3 nm) were made and used in this work. Templates of comparable film thickness values (PS $\sim$4200 nm and silica $\sim$4300 nm) were formed on F-doped tin oxide (FTO) coated glass. A standard cleaning procedure was employed to obtain pristine surfaces for subsequent template formation [27]. Films of polystyrene microspheres were deposited on FTO glass by a vertical convective self-assembly method [36]. Silica colloidal crystal templates were assembled using a method previously [37].

2.2. *Solution infiltration of colloidal crystal templates*

A procedure described elsewhere for TiO_2 deposition was adapted for use in the present study [38]. A Mettler Toledo MA 235 pH/ion analyser and InLab 413 electrode were used to record solution pH. Templates were immersed vertically in a solution containing $(NH4)_2TiF_6$ (0.1 mol dm^{-3}) and H_3BO_3 (0.2 mol dm^{-3}) and maintained at 35°C for a period of 2 h. Templates were subsequently removed from the infiltration bath, rinsed with deionized water and dried at room temperature. A similar procedure was employed for CdS infiltration but using baths containing $CdCl_2$ (0.0109 mol dm^{-3}), thiourea (0.0146 mol dm^{-3}), ammonia (5.028 mol dm^{-3}) and NaOH (0.0235 mol dm^{-3}). After drying, the films were sintered for 0.5 h (TiO_2, 300°C; CdS 200°C) to densify and improve the crystallinity of as-deposited films. The cycle of infiltration-rinse-sintering was repeated 4 times, a procedure that assured complete infiltration. A final annealing step (TiO_2, 450°C; CdS 300°C, for 2 h) was found to improve film quality. Sintering and annealing were conducted under static conditions in air using a heating rate of 1°C min^{-1}. Removal of silica templates was achieved by immersion of films in freshly

prepared aqueous NaOH solutions (~20% w/v) for 16 h at 80°C. Elimination of PS templates occurs during sintering.

2.3. *Characterisation studies*

X-ray diffraction studies were performed using secondary graphite monochromated Cu Ka radiation (40 kV) on either a Philips X'Pert Materials Diffractometer (APD) or Bruker AXS D8 diffractometer. Scanning electron microscopy (SEM) on carbon-coated films was performed using a Philips Excel 30 FEG SEM instrument. TEM electron microscopy and energy dispersive X-ray analysis (EDAX) were accomplished using a Philips CM200 (200 kV) microscope. TEM specimens were mounted on a carbon-coated copper TEM grid. Electronic absorption spectra were obtained using a Varian Cary 5000 UV-vis-NIR instrument.

3. Results and discussion

In preliminary work, a comparison of PS and SiO_2 colloidal templates was made in order to determine to most promising route towards reproducible films. Both systems have been employed previously for the fabrication of negative-replica macroporous films. However, small changes in reported synthetic procedures and the novel nature of the subsequent CBD infiltration approach made it necessary to firmly establish the merits and drawbacks of both systems. In general, PS has the advantage over SiO_2 of easier removal, by thermal or chemical methods, to yield the inverted template structure. However, SiO_2 structures are more robust and sintering of PS templates frequently results in significant shrinkage of the inverted framework, producing a large density of cracks and other defects in the macroporous network.

It was apparent that both PS and SiO_2 colloidal systems were successful for the preparation of well-ordered, macroporous template layers on substrates. Micrographs obtained from both systems are shown in figure 1. The close-packed arrangement of the colloidal crystals is clearly evident. Subsequently the efficiency of CBD infiltration processes for both template systems was assessed. Primary issues of concern included: what effect the infilling process had on the resilience of the template; the extent of pore filling and what were the chemical processes involved. It was apparent from early results that SiO_2 templates grown on substrates were more robust to the chemical infill processing and were thus superior to PS templates, which detached from substrates with extended infiltration time. Moreover, complete infiltration could be routinely obtained using SiO_2 templates.

The effectiveness of infiltration observed using SiO_2 templates could be rationalised in terms of advantageous surface chemistry. The pH of point of zero charge (pH_{pzc}) [39] is an important factor that determines the initial interface behaviour of oxide materials in aqueous electrolytes. The hydroxylated siliceous surface is highly hydrophilic and provides a high concentration of available sorption sites for nucleation and growth processes in aqueous solution, in marked contrast to PS templates for which infiltration was markedly poorer. The results are shown in figure 2. After infiltration for 8 hours, in the PS case, the voids are not fully filled and the TiO_2 framework is dispersed and

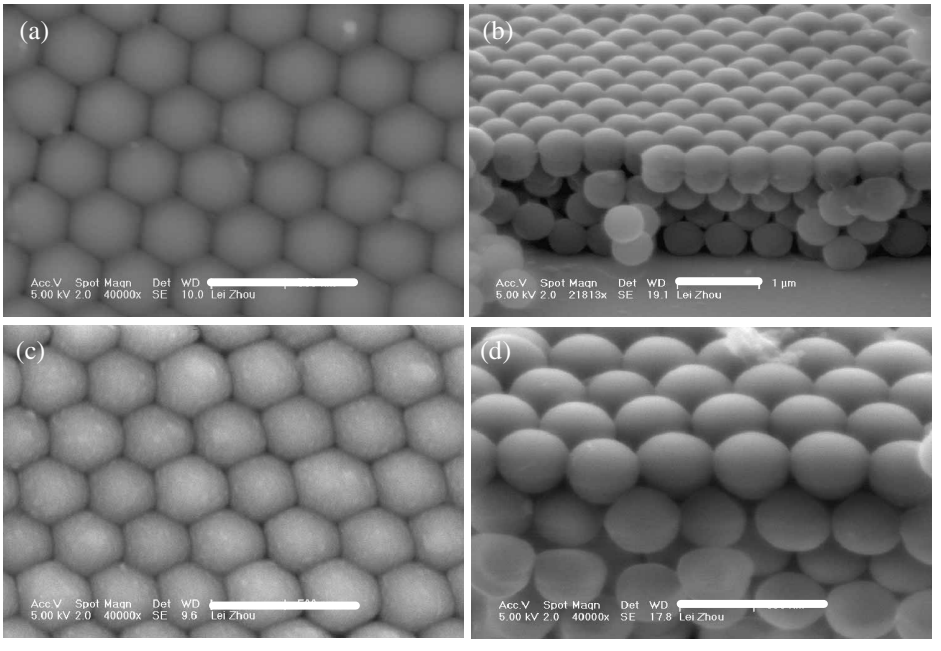

Figure 1. SEM images of colloidal crystal templates (scalebar = 1µm). (a, b) Top view and cross section of the 460 nm PS; (c, d) top view and cross section of the 435.5 nm SiO_2.

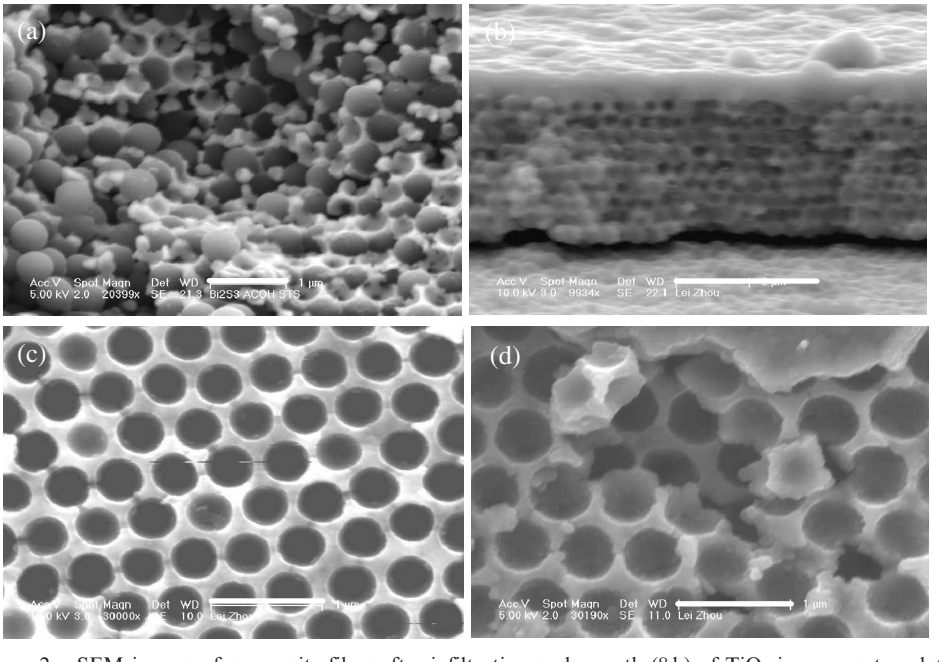

Figure 2. SEM images of composite films after infiltration and growth (8 h) of TiO_2 in porous templates (a) Polystyrene and (b) SiO_2 colloids. Removal of templates shown in (c) polystyrene and (d) SiO_2 leads to formation of macroporous films. Scalebar = 1 µm (4 µm for b).

not interconnected. After removing the template, only the initial monolayer on the substrate is remains intact. However for SiO_2 based templates, the voids are fully filled and the TiO_2 framework is complete and interconnected. Removal of the support templates reveals formation of multilayer TiO_2 macroporous films.

At solution pH ~12 and ~4.5 for CBD-CdS and CBD-TiO_2 respectively, the surface hydroxyl groups on silica template particles ($pH_{pzc} \approx 2$) will tend to be deprotonated and therefore receptive to absorption of cationic species. Values for the pH_{pzc} of TiO_2 (~6) and CdS (~12) imply that in the initial stages of infiltration, growth in both CBD systems will proceed via sorption of cationic species on deprotonated surface silanol groups. Furthermore we can assume the metathesis of surface "Cd-OH" to CdS in the presence of in-situ generated S^{2-} is efficient; we have previously shown identical baths deposit good quality films of CdS when formally supersaturated in hydroxy-cadmium species in solution [40].

The pattern of results suggests that infiltration by CBD methods is optimised by minimising homogeneous nucleation and growth processes. While complete infiltration of interconnected cavities within macroporous SiO_2 templates is often obtained, more reproducible results are obtained by using a series of short infill-rinse steps. Formation of colloidal material in deposition baths and surface sorption may ultimately lead to premature pore closure at the extremities of the colloidal crystal and thus compromise the infiltration process, as shown in figure 3. Thus effective infiltration can be realised by adjustment the deposition parameters to promote heterogeneous but minimise homogeneous nucleation and growth.

Upon establishment of a (few) monolayer(s) of infill material on colloidal template surfaces throughout the macroporous structure, further growth and infilling of pores relies upon controlled growth of material within increasingly restricted kinetic environments. However, we have reasoned that two enabling factors will assist the solution deposition process; firstly, capillary forces will tend to increase at contracting pore necks at the periphery of voids with time and secondly, the CBD method employs low viscosity aqueous solutions and thus benefits from better mass transport than sol-gel methods [41] for which large concentration gradients, due to localised depletion of reagents, are likely to retard growth processes in pores. In similar environments and using CBD methods, local supersaturation (a prerequisite for nucleation) is likely to be maintained at a moderate level, appropriate for heterogeneous growth but below that for which homogeneous processes may operate. The surface charge density is also

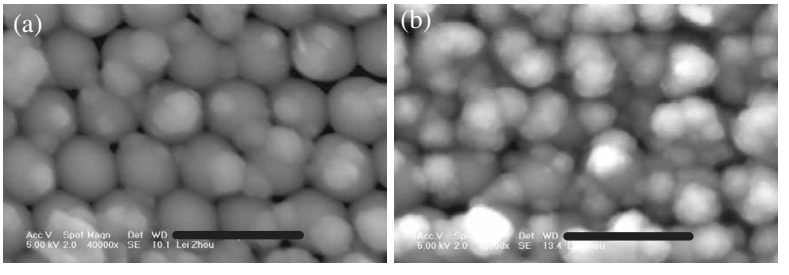

Figure 3. SEM images of SiO_2 templates after infiltration by TiO_2. (a) Two infill-rinse-sinter circles; (b) single step infiltration (4 h) and rinse-sinter steps. Scalebar = 1 μm.

expected to rise in regions where there is larger surface curvature; the significance of the phenomenon is difficult to factor but does not appear to negate our simple approach.

By employing a series of sequential, short infill/rinse/anneal steps, the formation of precipitous materials (common for CBD processes with extended reaction times) is minimised, removal of any deleterious reaction products ensured and the crystallinity and integrity of the macroporous structure enhanced. The evolution of the inverse replica structure as a function of infill cycles is represented in figure 4. The efficiency of the infiltration process is clearly demonstrated, growth appears to occur in a conformal manner and evidently, the pore channels at extremities of the porous colloidal crystal remain open throughout the procedure. Complete infiltration and surface planarisation is obtained after four infill-rinse-sinter processes. Removal of the SiO_2 template yields thin film macroporous structures showing good long-range periodicity over a large area (figure 5). We are currently optimising the thermal processing conditions in order to minimise the formation of structural defects such as cracks, which compromise the isotropic long-range order in the film.

Delaminated material was investigated by TEM in order to probe the internal structure of films. Further evidence for long-range order in the macroporous CdS and

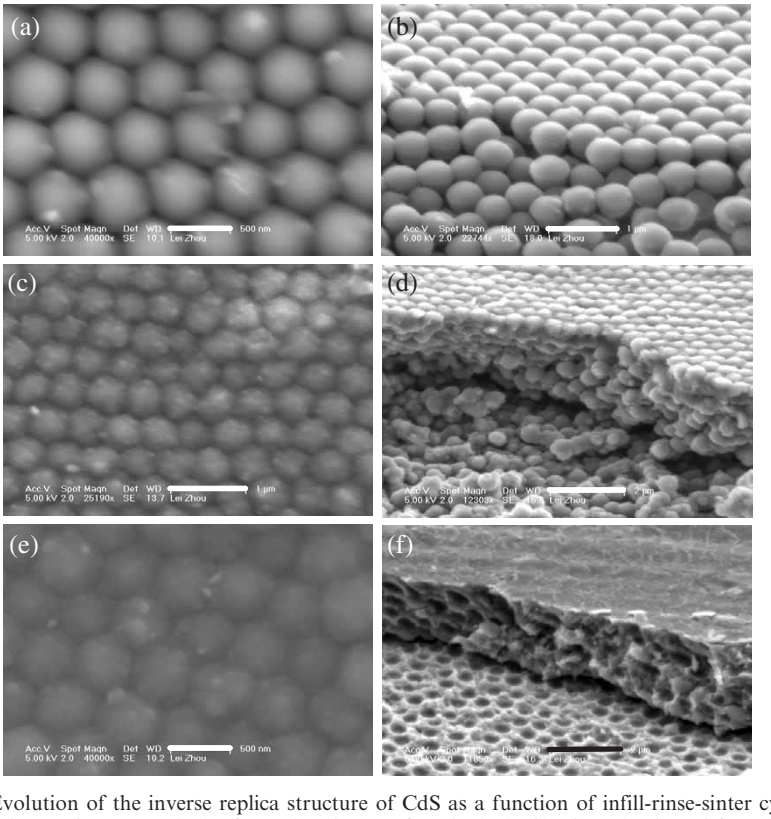

Figure 4. Evolution of the inverse replica structure of CdS as a function of infill-rinse-sinter cycles. SEM images (top view and cross section) of template layers after single (a, b), three (c, d) and four (e, f) cycles. Scalebar = 0.5 μm (a, e); 1 μm (b, c); 2 μm (d, f).

TiO_2 inverse replica films was obtained; the close-packed arrangement of pores in the inverse replica structure is clearly represented in figure 6. Images collected by HR-TEM and SAED methods indicated the infill material was hexagonal phase CdS (JCPDS 02-0563) and polycrystalline anatase (JCPDS 86-1156) comprising grains of diameter ca. 4–7 nm. Moreover, no signals for Si were detected in EDX of TiO_2 macroporous films, consistent with efficient removal of template material. The crystallinity and phase identity were confirmed by XRD measurements, representative diffractograms are given in figure 7.

Electronic spectra of macroporous films provide good evidence for photonic behaviour. A characteristic property of photonic crystals is the appearance of stop-bands for light propagation due to coherent Bragg scattering, usually termed a photonic bandgap (PBG). Photonic materials require large and periodic refractive index contrast (i.e. n_2/n_1 where n_1 and n_2 refer to the small and large components of refractive index in the structure), identical for all light directions. In addition, negligible absorption of light photons in the vis-NIR region is required for a full PBG in a material with practical applications. As the absorption edge is proportional to the fourth power of the refractive index (RI) for semiconductors, choice of suitable materials with sufficiently large RI and electronic bandgap is restricted.

A photonic stop-band occurs when the refractive index contrast is incomplete and leads to production of a pseudo-PBG (i.e. optical stop-bands restricted to specific crystal directions) rather than full PBG. In the present work, useful information was

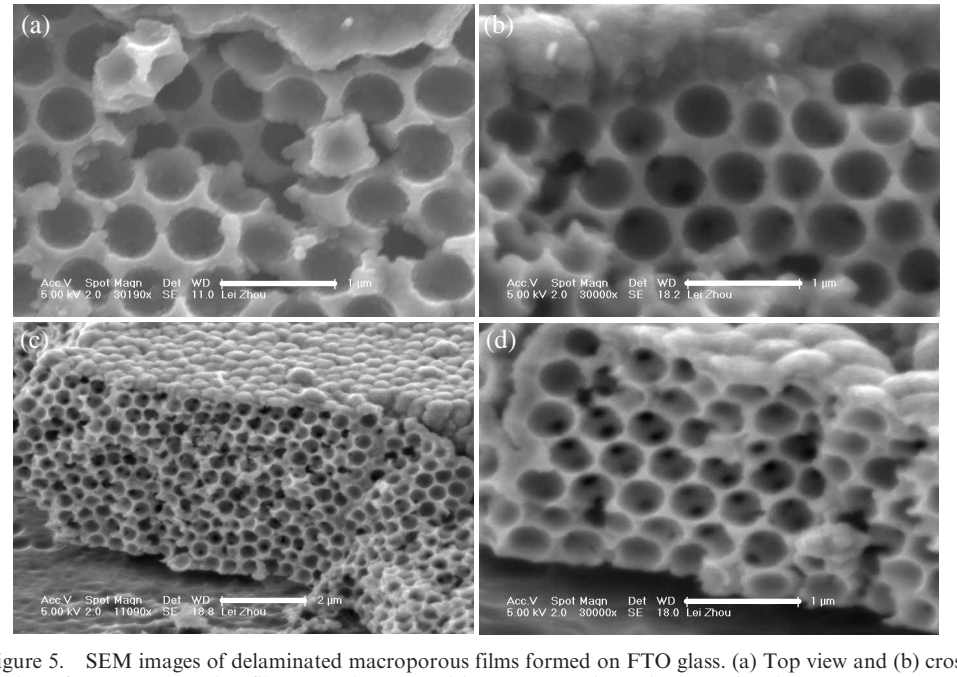

Figure 5. SEM images of delaminated macroporous films formed on FTO glass. (a) Top view and (b) cross section of macroporous TiO_2 films (template comprising 523.5 nm SiO_2 spheres) and (c) low mag. (×11K) and (d) high mag. (×30K) cross section of macroporous CdS films (template comprising 435.5 nm SiO_2 spheres). Scalebar = 1 µm (a, b, d); 2 µm (c).

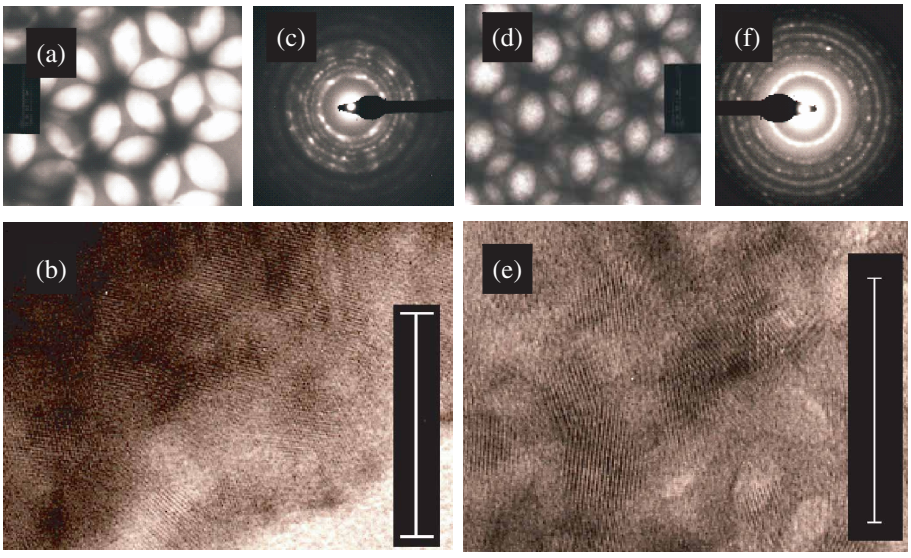

Figure 6. TEM images of macroporous CdS films. (a) low resolution image; (b) high resolution image, scale bar is 20 nm; (c) SAED pattern of area shown in (b): TEM images of macroporous TiO_2 films; (d) low resolution image; (e) high resolution image, scale bar is 20 nm; (f) SAED pattern of area shown in (e).

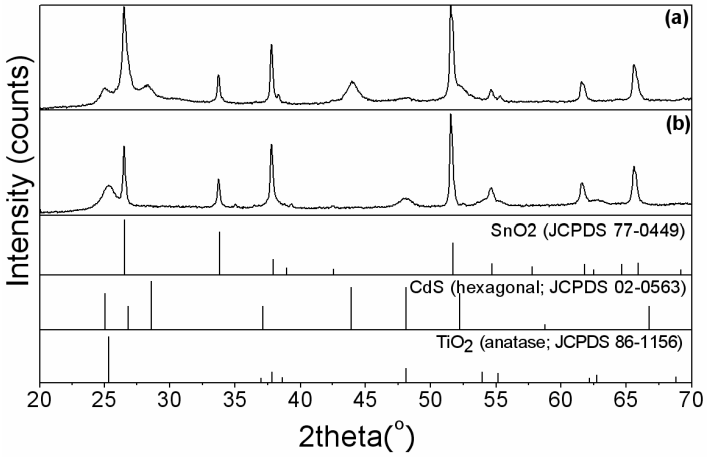

Figure 7. XRD patterns obtained for macroporous (a) CdS films and (b) TiO_2 on FTO glass.

gained by assessing the shift in the stop-band as a function of degree of infiltration of SiO_2 colloidal template layers (435.5 nm diameter). Increase in the dielectric contrast results in a bathochromic shift of the stop-band position. Measurements were conducted in transmission mode, where stops-bands appear as a dip in the recorded spectrum. Results appeared to confirm complete infiltration was obtained after four infill cycles.

Representative transmission spectra are shown in figure 8. Simple treatment of data provided clear evidence that using CBD infiltration methods, macroporous CdS and TiO_2 thin films on FTO supports, which behave as inverse opals, can be fabricated. It has been previously shown for identical close-packed synthetic opals that the principle feature observed in optical spectra is associated with Bragg reflection from the (111) planes. The position of the stop-band is given by equation (1) [42]

$$\lambda_{111} = 2\left(\frac{2}{3}\right)^{0.5} D(n_e^2 - \sin^2\theta)^{0.5} \quad (1)$$

where λ_{111} is the wavelength of the stop-band (nm), D is the diameter of the colloidal spheres (nm), θ is the incidence angle and n_e is the effective refractive index of the film. In the linear approach [43], the square of effective refractive index can be determined as follows:

(1) During the infiltration process, air within templates is gradually replaced by CdS with increasing infilling cycles. The film is composed of air, CdS and SiO_2.

$$n_e^2 = (0.26 - f)\, n_{air}^2 + 0.74 n_{SiO_2}^2 + f\, n_{CdS}^2 \quad (2)$$

(2) Upon removal of the templates, SiO_2 is substituted by air and an inverse replica film of CdS with air voids is formed.

$$n_e^2 = (1 - f) n_{air}^2 + f n_{CdS}^2 \quad (3)$$

where $n_{air} = 1$, $n_{SiO_2} = 1.45$ and $n_{CdS} = 2.6$; f is the CdS filling fraction relative to the total volume of the opal and lies between 0 (opal template) and 0.26 (fully infiltrated opal). This parameter is used to estimate the extent of semiconductor infiltration.

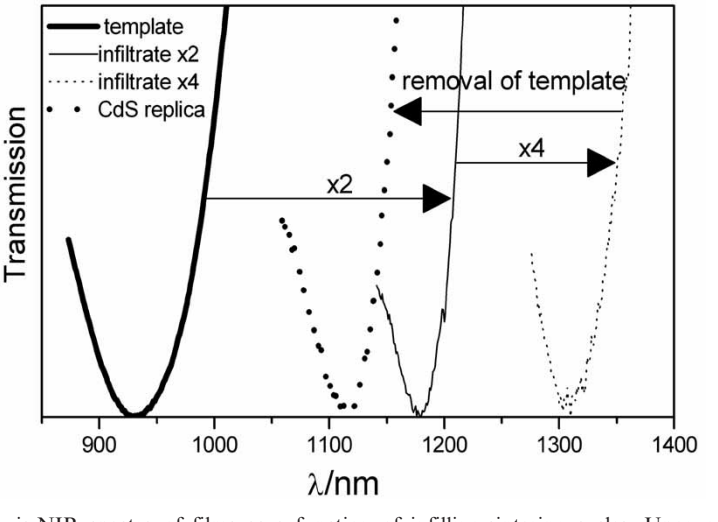

Figure 8. UV-vis-NIR spectra of films as a function of infilling-sintering cycles. Upon removal of the template, a CdS inverse-opal replica is produced.

Table 1. Bragg peak position as a function of CdS infiltration cycles in macroporous silica for a sample comprising 435.5 nm diameter spheres.

Number of infiltrations	Peak position λ_{111} (nm)	Filling fraction f
Template alone[a]	968	0
Two cycles	1178	0.17
Four cycles	1310	0.28
Final inverse opal[b]	1115	0.27

[a] Predicted λ_{111} (ideal f.c.c. structure, $f = 0$) is 957 nm.
[b] Predicted λ_{111} ($f = 0.26$; complete infiltration) = 1122 nm.

Table 1 shows the relationship between measured λ_{111} for normal incidence ($\theta = 0$) and the CdS filling fraction, f, calculated through equations (1)–(3) for the samples at different stages. It is very clear that after four short infill/rinse/anneal circles, the voids are fully filled by the CdS, and the inverse CdS replica grown in templates is entirely retained without damage after removal of the templates. The apparent overfilling ($f > 0.26$) derives from the presence of a surface layer in regions of the film probed via the spectrometer, which would tend to increase $n_{effective}$, λ_{111} (nm) and thereby the calculated f value.

In summary we have employed simple low temperature CBD methods to achieve complete infiltration of SiO_2 opal thin films with CdS and TiO_2. The effectiveness of the approach is rationalised in terms of promotion of heterogeneous, rather than homogeneous, nucleation and growth processes under conditions of low solution viscosity and moderate supersaturation. Removal of templates allows fabrication of highly crystalline, robust, macroporous inverse replica structures. Preliminary optical studies of films indicate that periodic modulation of dielectric behaviour is obtained, with potential use for photonic applications. Moreover, because of the similarity to conventional CBD methods, this strategy can be widely used to produce macroporous films composed of other sulfides and oxides which have been successfully deposited on glass by conventional CBD methods, without substantial modification. This approach also has potential for fabrication of more complex structures, *e.g.* multilayer macroporous films composed of different semiconductors.

4. Conclusions

We have employed simple CBD methods to effect complete infiltration of SiO_2 opal thin films with CdS and TiO_2. Removal of templates allows fabrication of macroporous inverse replica structures that exhibit periodic modulation of dielectric behaviour.

Acknowledgements

The authors thank the EPRSC, ORS and University of Manchester for funding this work.

References

[1] Manual of Symbols and Terminology for Physicochemical Quantities and Units Appendix II—Definitions, Terminology and Symbols in Colloid and Surface Chemistry Part I. *Pure and Applied Chemistry*, **31**, 585 (1972).

[2] D.B. Akolekar, A.R. Hind, S.K. Bhargava. Synthesis of macro-, meso-, and microporous carbons from natural and synthetic sources, and their application as adsorbents for the removal of quaternary ammonium compounds from aqueous solution. *J. Colloid Interface Sci.*, **199**, 92 (1998).

[3] K. Lewandowski, P. Murer, F. Svec, J.M.J. Frechet. The design of chiral separation media using monodisperse functionalized macroporous beads: effects of polymer matrix, tether, and linkage chemistry. *Anal. Chem.*, **70**, 1629 (1998).

[4] B.T. Holland, L. Abrams, A. Stein. Dual templating of macroporous silicates with zeolitic microporous frameworks. *J. Am. Chem. Soc.*, **121**, 4308 (1999).

[5] B.T. Holland, C.F. Blanford, A. Stein. Synthesis of macroporous minerals with highly ordered three-dimensional arrays of spheroidal voids. *Science*, **281**, 538 (1998).

[6] O.D. Velev, E.W. Kaler. Structured porous materials via colloidal crystal templating: from inorganic oxides to metals. *Adv. Mater.*, **12**, 531 (2000).

[7] Y.A. Vlasov, X.Z. Bo, J.C. Sturm, D.J. Norris. On-chip natural assembly of silicon photonic bandgap crystals. *Nature*, **414**, 289 (2001).

[8] J. Wijnhoven, W.L. Vos. Preparation of photonic crystals made of air spheres in titania. *Science*, **281**, 802 (1998).

[9] S.H. Park, Y.N. Xia. Macroporous membranes with highly ordered and three-dimensionally interconnected spherical pores. *Adv. Mater.*, **10**, 1045 (1998).

[10] P. Jiang, K.S. Hwang, D.M. Mittleman, J.F. Bertone, V.L. Colvin. Template-directed preparation of macroporous polymers with oriented and crystalline arrays of voids. *J. Am. Chem. Soc.*, **121**, 11630 (1999).

[11] M.E. Abdelsalam, P.N. Bartlett, J.J. Baumberg, S. Coyle. Preparation of arrays of isolated spherical cavities by self-assembly of polystyrene spheres on self-assembled pre-patterned macroporous films. *Adv. Mater.*, **16**, 90 (2004).

[12] P.N. Bartlett, J.J. Baumberg, S. Coyle, M.E. Abdelsalem. Optical properties of nanostructured metal films. *Faraday Discuss Chem. Soc.*, **125**, 117 (2004).

[13] P.N. Bartlett, M.A. Ghanem, I.S. El Hallag, P. De Groot, A. Zhukov. Electrochemical deposition of macroporous magnetic networks using colloidal templates. *J. Mater. Chem.*, **13**, 2596 (2003).

[14] J.S. King, E. Graugnard, C.J. King. TiO_2 Inverse opals fabricated using low-temperature atomic layer deposition. *Adv. Mater.*, **17**, 1010 (2005).

[15] S. Kuai, S. Badilescu, G. Bader, L. Brüning, X.F. Hu, V.V. Truong. Preparation of large-area 3D ordered macroporous titania films by silica colloidal crystal templating. *Adv. Mater.*, **15**, 73 (2003).

[16] M.E. Turner, T.J. Trentler, V.L. Colvin. Thin films of macroporous metal oxides. *Adv. Mater.*, **13**, 180 (2001).

[17] G. Subramanian, V.N. Manoharan, J.D. Thorne, D.J. Pine. Ordered Macroporous materials by colloidal assembly: a possible route to photonic bandgap materials. *Adv. Mater.*, **11**, 1261 (1999).

[18] F.Q. Tang, H. Fudouzi, Y. Sakka. Fabrication of macroporous alumina with tailored porosity. *J. Am. Ceram. Soc.*, **86**, 2050 (2003).

[19] P.N. Bartlett, P.R. Birkin, M.A. Ghanem. Electrochemical deposition of macroporous platinum, palladium and cobalt films using polystyrene latex sphere templates. *Chem. Commun.*, **17**, 1671 (2000).

[20] P.V. Braun, P. Wiltzius. Electrochemically grown photonic crystals. *Nature*, **402**, 603 (1999).

[21] A. Blanco, H. Míguez, F. Meseguer, C. López, F. López-Tejeira, J. Sánchez-Dehesa. Photonic band gap properties of CdS-in-opal systems. *Appl. Phys. Lett.*, **78**, 3181 (2001).

[22] B.H. Juarez, S. Rubio, J. Sánchez-Dehesa, C. López. Antimony trisulfide inverted opals: growth, characterisation and photonic properties. *Adv. Mater.*, **14**, 1486 (2002).

[23] G. Hodes. *Chemical Solution Deposition of Semiconductor Films*, Marcel Dekker, London (2002).

[24] D.S. Boyle, A. Bayer, M.R. Heinrich, O. Robbe, P. O'Brien. Novel approach to the chemical bath deposition of chalcogenide semiconductors. *Thin Solid Films*, **361–362**, 150 (2000).

[25] D.S. Boyle, S. Hearne, D.R. Johnson, P. O'Brien. A study of impurities in some CdS/CdTe photovoltaic cells prepared by wet-chemical methods using secondary ion mass spectrometry and X-ray photoelectron spectroscopy. *J. Mater. Chem.*, **9**, 2879 (1999).

[26] D.S. Boyle, P. O'Brien, D.J. Otway, O. Robbe. Novel approach to the deposition of CdS by chemical bath deposition: the deposition of crystalline thin films of CdS from acidic baths. *J. Mater. Chem.*, **9**, 725 (1999).

[27] A. Bayer, D.S. Boyle, P. O'Brien. In-situ kinetic studies of the chemical bath deposition of zinc sulphide from acidic solutions. *J. Mater. Chem.*, **12**, 2940 (2002).

[28] P. O'Brien, D.J. Otway, D. Smyth-Boyle. The importance of ternary complexes in defining basic conditions for the deposition of ZnS by aqueous chemical bath deposition. *Thin Solid Films*, **361–362**, 17 (2000).
[29] K. Govender, D.S. Boyle, P. O'Brien. Developing cadmium-free window layers for solar cell applications: some factors controlling the growth and morphology of β-indium sulfide thin films and related (In,Zn)S ternaries. *J. Mater. Chem.*, **13**, 2242 (2003).
[30] D.S. Boyle, K. Govender, P. O'Brien. Novel low temperature solution deposition of perpendicularly orientated rods of ZnO: substrate effects and evidence of the importance of counter-ions in the control of crystallite growth. *Chem. Commun.*, **1**, 80 (2002).
[31] K. Govender, D.S. Boyle, P.B. Kenway, P. O'Brien. Understanding the factors that govern the deposition and morphology of thin films of ZnO from aqueous solution. *J. Mater. Chem.*, **14**, 2575 (2004).
[32] K. Govender, D.S. Boyle, P. O'Brien, D. Binks, D. West, D. Coleman. Room-temperature lasing observed from ZnO nanocolumns grown by aqueous solution deposition. *Adv. Mater.*, **14**, 1221 (2002).
[33] D.S. Boyle, K. Govender, P. O'Brien. Novel wet-chemical routes to nano- and microstructured semiconductor layers for improved efficiency photovoltaic devices. *Thin Solid Films*, **431–432**, 483 (2003).
[34] D. Berhanu, D.S. Boyle, K. Govender, P. O'Brien. Novel wet-chemical routes to highly structured semiconductor layers for improved efficiency photovoltaic devices. *J. Mater. Sci: Mat. Elect.*, **14**, 579 (2003).
[35] W. Stöber, A. Fink, E. Bohn. Controlled growth of monodisperse silica spheres in the micron size range. *J. Colloid Interface Sci.*, **26**, 62 (1968).
[36] A.S. Dimitrov, K. Nagayama. Continuous convective assembling of fine particles into two-dimensional arrays on solid surfaces. *Langmuir*, **12**, 1303 (1996).
[37] S. Wong, V. Kitaev, G.A. Ozin. Colloidal crystal films: advances in universality and perfection. *J. Am. Chem. Soc.*, **125**, 15589 (2003).
[38] S. Deki, Y. Aoi, O. Hiroi, A. Kajinami. Titanium(IV) Oxide thin films prepared from aqueous solution. *Chem. Lett.*, **6**, 433 (1996).
[39] I. Larson, P. Attard. Surface charge of silver iodide and several metal oxides. Are all surfaces nernstian?. *J. Colloid. Interface. Sci.*, **227**, 152 (2000).
[40] P. O'Brien, T. Saeed. Deposition and characterization of cadmium sulfide thin films by chemical bath deposition. *J. Cryst. Growth*, **158**, 497 (1996).
[41] S.L. Kuai, X.F. Hu, V.V. Truong. Synthesis of thin film titania photonic crystals through a dip-infiltrating sol–gel process. *J. Cryst. Growth*, **259**, 404 (2003).
[42] P.L. Flaugh, S.E. O'Donnell, S.A. Asher. Development of a new optical wavelength rejection filter; demonstration of its utility in Raman spectroscopy. *Appl. Spectrosc.*, **38**, 847 (1984).
[43] R. Torrecillas, A. Blanco, M.E. Brito, C. López, H. Míguez, F. Meseguer, J.S. Moya. Microstructural study of CdS/Opal composites. *Acta. Mater.*, **48**, 4653 (2000).